

Slope stability analysis on a regional scale using GIS: a case study from Dhading, Nepal

Ram Ray


Environmental geology

Cite this paper

Downloaded from [Academia.edu](#) 

[Get the citation in MLA, APA, or Chicago styles](#)

Related papers

[Download a PDF Pack](#) of the best related papers 



[Regional landslide susceptibility: spatiotemporal variations under dynamic soil moisture cond...](#)

Ram Ray

[Impacts of Unsaturated Zone Soil Moisture and Groundwater Table on Slope Instability](#)

Ram Ray

[Relationships among remotely sensed soil moisture, precipitation and landslide events](#)

Ram Ray

Slope stability analysis on a regional scale using GIS: a case study from Dhading, Nepal

R. L. Ray · F. De Smedt

Received: 31 January 2008 / Accepted: 11 June 2008 / Published online: 28 June 2008
© Springer-Verlag 2008

Abstract A spatially distributed physically based slope stability model combined with a hydrological model is presented and applied to a 350-km² area located in Dhading district, Nepal. Land slide safety factor maps are generated for five cases, including three steady state conditions assuming either completely dry soils, half saturated soils, or fully saturated soils, and two quasi-dynamic conditions, i.e. soil wetness resulting from storm events with, respectively a 2 or 25-year return period. For the quasi-dynamic cases, two methods are used, one based on accumulation of groundwater flow from upstream areas, and the other on accumulation of soil water from direct infiltration. The methodology delineates areas most prone to shallow land sliding in function of readily available data as topography, land-use and soil types. For the study area only 29% of the soils are unconditionally stable, while 25% of the soils are found to be unstable under fully saturated conditions. The comparison between the methods based on contributing area or on infiltration for quasi-dynamic conditions show that the approach based on infiltration is more reliable for the study area. The proposed methodology for predicting landslide susceptibility on a regional scale, based on basic data in GIS form, may be useful for other remote regions where detailed information is not available.

Keywords Slope stability · Landslide · GIS analysis · Wetness index · Nepal

Introduction

Geotechnical slope stability analysis is commonly used for assessing the stability of slopes with uncontrolled or controlled groundwater or pore water pressure. In all these situations, hillslopes that are, at least in part, saturated with groundwater will be subjected to seepage-induced body forces, and thus to potentially de-establishing effects (Windisch 1991). The emphasis therefore should lie on understanding the groundwater dynamics in the system, in order to assess its impact on the stability of the slopes. When planning land-use activities, it is important to consider the risks posed by slope instability (and eventually landslides) and also to account for the potential effects of the land-use on the geo-hydrology of the slopes and on landslide activity.

Landslides cause significant problems in mountainous countries like Nepal, often aggravated by rapid and uncontrolled development. In recent years, many studies have been carried out related to landslide hazard and risk assessment in the Himalayan region. Several approaches have been presented, including the landslide hazard evaluation factor (Anbalagan 1992; Anbalagan and Singh 1996), the mountain risk engineering approach of Deoja et al. (1991), GIS based rating techniques (Thapa and Dhital 2000; Dhital 2000; Saha et al. 2002; Sarkar and Kanungo 2004), statistical techniques (Skirikar et al. 1998; Dhakal et al. 1999; Pathak and Nilsen 2004), deterministic techniques (Joshi et al. 2000), and the landslide risk assessment of Petley et al. (2004).

In many of these studies extensive use is made of remote sensing and geographic information systems (GIS). As more and more data become available in digitised format, it becomes possible to develop software routines that can perform slope stability analysis in conjunction with GIS. GIS methods for modelling slope instability have been

R. L. Ray · F. De Smedt (✉)
Department of Hydrology and Hydraulic Engineering,
Vrije Universiteit Brussel, Pleinlaan 2,
1050 Brussels, Belgium
e-mail: fdesmedt@vub.ac.be

employed by different investigators throughout the world. Reviews and outlines of the methods are given by Varnes (1984), Hansen (1984), van Westen (1994), Bonham-Carter (1994), Carrara et al. (1995), Hutchinson (1995), Soeters and van Westen (1996), van Westen et al. (1997), Aleotti and Chowdhury (1999), Guzzetti et al. (1999), Gorsevski et al. (2003).

In this study, we will focus on physically based slope stability modelling and the influence of rainstorm events incorporating spatial heterogeneity of variables as soil type and topography. The aim of this study is to investigate a methodology for the generation of landslide safety factor maps on a regional scale and to produce landslide susceptibility maps of the study area. The results may help to predict the spatial distribution of landslides which is essential in future land-use planning.

Theory

A wide variety of methods have been developed for slope stability analysis on a regional scale (e.g. Montgomery and Dietrich 1994; van Westen and Terlien 1996; Burton and Bathurst 1998; Pack et al. 1998, 2001; Borga et al. 2002; Saha et al. 2002; Dhakal and Sidle 2004). A slope stability factor can be calculated by the infinite slope method (Skempton and DeLory 1957), which expresses the ratio of stabilising to destabilising forces. A schematic representation of the different variables is given in Fig. 1, adapted from Skempton and DeLory (1957). The stability factor has been adapted by several investigators (e.g. Montgomery and Dietrich 1994; van Westen and Terlien 1996; Acharya et al. 2006) as

$$F = \frac{C_s + C_r}{\gamma_e D \sin \theta} + \left(1 - m \frac{\gamma_w}{\gamma_e}\right) \frac{\tan \phi}{\tan \theta} \quad (1)$$

where, F is the slope stability factor (adimensional), C_s and C_r are the effective soil and root cohesion (kN/m^2), D is the

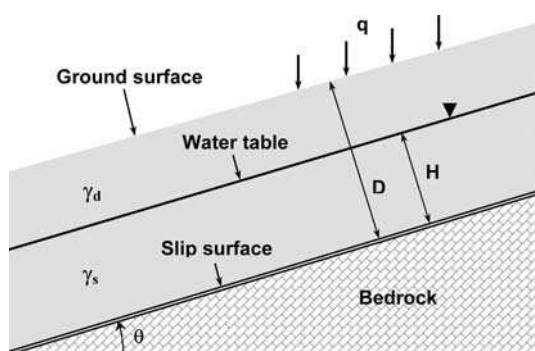


Fig. 1 Schematic representation of the infinite slope method depicting the different parameters and variables (adapted from Skempton and DeLory 1957)

Table 1 Slope stability classes

Safety factor	Slope stability class	Remarks
$F > 1.5$	Stable	Only major destabilising factors lead to instability
$1.25 < F < 1.5$	Moderately stable	Moderate destabilising factors lead to instability
$1 < F < 1.25$	Quasi stable	Minor destabilising factors can lead to instability
$F < 1$	Unstable	Stabilising factors are needed for stability

depth of the soil above the failure plain (m), ϕ is the angle of internal friction of the soil ($^\circ$), θ is the slope angle ($^\circ$), γ_w is the unit weight of water (kN/m^3), and γ_e is the effective unit weight of the soil (kN/m^3) as defined by van Westen and Terlien (1996), as

$$\gamma_e = q \cos \theta / D + (1 - m) \gamma_d + m \gamma_s \quad (2)$$

where γ_d is the unit weight of the dry soil (kN/m^3) and γ_s is the unit weight (kN/m^3) of the saturated soil, and q is any additional load on the soil surface (kN/m^2). Parameter m corresponds to the wetness index and theoretically expresses the relative position of the water table H/D , where H is the saturated thickness of the soil above the failure plain (m) and D is the total depth of the soil above the failure plain (m).

Whether a slope is stable or unstable depends on the values of F being larger or smaller than one, and different stability classes can be defined based on the value of F . In this study, we will use stability classes as presented in Table 1: slopes are denoted as unstable in case the safety factor F is smaller than 1, quasi stable if F is between 1 and 1.25, moderately stable if F is between 1.25 and 1.5, and stable if F is larger than 1.5. The stability is predominantly depending upon the value of the soil cohesion and friction angle. However, the saturated index has a pronounced influence on the stability condition. The most favourable condition towards stability is a completely dry soil ($m = 0$), and the worst condition is a completely saturated soil ($m = 1$).

The triggering mechanism for slope instability is usually a rise of the groundwater table, which increases soil saturation and ultimately the pore water pressure and consequently reduces the normal effective stresses and shear strength for potential failure surfaces. Simple models have been developed for estimating the soil saturation index based on the hillslope topography (e.g. Montgomery and Dietrich 1994; Borga et al. 1998; Pack et al. 1998). These approaches are based on the assumption that the throughflow is parallel to the ground surface and equal to the total infiltration of rainfall in the upstream area. Hence,

the first assumption implies that the subsurface flow in the saturated part of the soil profile can be expressed by Darcy’s law as $KH\sin\theta$, where K is the hydraulic conductivity (m/s) of the soil, H the saturated depth of soil (m) also represents the thickness of the groundwater layer, and $\sin\theta$ is the hydraulic gradient (decline in water table elevation per unit length in the flow direction, as seen in Fig. 2), while the second assumption implies that

$$(KH \sin \theta)B = IA \tag{3}$$

where B is the width of the considered subsurface flow section (m), I is the infiltration or effective precipitation intensity (m/s), and A is the upstream contributing area (m^2). Equation 3 enables to calculate the saturated thickness, H , as a function of the other variables and to obtain an expression of the soil saturation index as

$$m = \frac{H}{D} = \frac{IA_s}{KD \sin \theta} \tag{4}$$

where $A_s = A/B$ is the specific contributing area, that is the contributing area per considered subsurface flow section. Equation 4 is based on the assumption that all the infiltrating water in the upstream contributing area contributes to the groundwater flow at the downstream convergence point. It does not take into account the time period for the flow accumulation or the storage and delay in the upstream area. Hence, whatever the time period, it is assumed that the whole upstream area is contributing instantaneously to the groundwater flow in any downstream section. In addition the validity of the assumption is obviously not valid in terrains with

permeable bedrock. In reality, due to slow groundwater movement, it is probably more realistic to assume that all infiltrating water is stored by a rise of the water table before subsurface flow occurs. The amount of water stored, ΔS (m), per increase in water table elevation, ΔH , is known as the specific yield (or effective porosity), $\alpha = \Delta S/\Delta H$ (adimensional) (De Smedt 2006). Hence, starting from an initial water table elevation H_0 , the wetness index after a rain event can be derived as

$$m = \frac{H_0 + \Delta H}{D} = \frac{H_0}{D} + \frac{\Delta S}{\alpha D} = m_0 + \frac{I\Delta t \cos \theta}{\alpha D} \tag{5}$$

where $m_0 = H_0/D$ is the initial wetness index before the rainfall event, and the amount of infiltrated rainfall stored in the soil is given by $\Delta S = (\cos\theta)I\Delta t$. Δt is the duration of the storm (s) and $\cos\theta$ compensates for the fact that rain intensities are equated on a horizontal area basis while the soil surface has a slope angle θ . Of course, wetness values equated with Eq. 5 are restricted to be smaller or equal to one. On the basis of Eq. 5, the wetness index after a rainfall event can be generated on a regional scale. The choice for the initial wetness index (m_0) remains to be decided by the user, based on the antecedent soil moisture and rainfall conditions, and the level of confidence that the user intends to accept or impose on the slope stability analysis. The higher the values for m_0 , the more conservative will be the stability models. In the present application, we will take a cautious approach and assume average initial moisture conditions, i.e. the soil is half saturated, or $m_0 = 0.5$, at the start of the considered rainfall event.

Fig. 2 Location and main characteristics of the study area in the Dhading district of Nepal

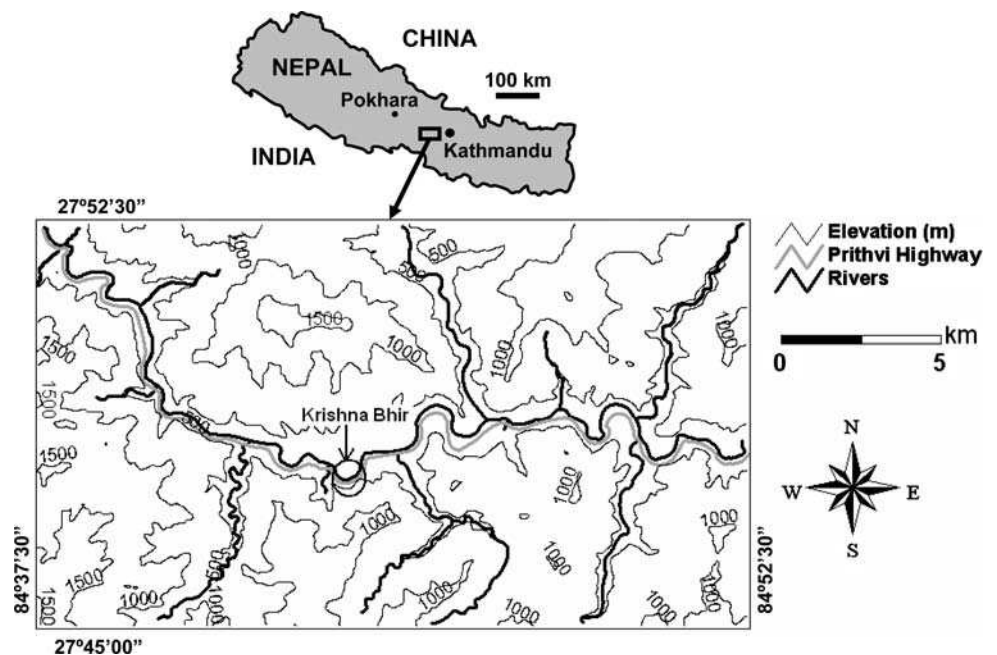




Fig. 3 Photograph of the study area showing the Trisuli River, the river valley and bordering mountains; the picture was taken in 2004

Application

Nepal is located in the heart of the Himalayas and occupies nearly one-third of the mountain range. About 83% of the country is mountainous terrain, and the remaining 17% in the south are alluvial plains. The study area, shown in Fig. 2, is situated in Dhading, one of the 75 districts of Nepal. The transnational Prithvi highway connecting Kathmandu and Pokhara runs through the southern part of the district. The road parallels the Trisuli River. Figure 3 shows a general view of the study area, with the Trisuli River valley flanked by mountain ranges. The investigated area is about 25 by 14 km (350 km²), with altitudes ranging from about 240 to 1,920 m above sea level. Landslides occur frequently in this area during the monsoon season from July to September, usually leading to interruption of the traffic. One of the major landslides in the district initiated in 2000 (Dahal et al. 2006) and became catastrophic in 2003 along the Prithvi highway at Krishna Bhir, indicated in Fig. 2 and depicted in Fig. 4 (“bhir” is the Nepali word for steep slope). In total eight landslides were observed along the Prithvi highway during the monsoons from 2000 to 2004. Field observations showed that these landslides were shallow and mostly translational in nature, with widths from 10 to 100 m and lengths of 10–300 m (Dahal 2004; Dahal et al. 2006).

The topographical map, scale 1:25,000, (Department of Survey, Ministry of Land Reforms, Nepal, 1992) was digitised and transformed into a digital elevation model (DEM) with a grid size of 20 by 20 m. A slope angle map of the study area was derived from this DEM. Slope angles vary from 0° to 61° with an average value of 30.5°. Similarly, the 1:50,000 scale land-use map (Department of Survey, Ministry of Land Reforms, Nepal, 1984) was digitised to raster form with the same cell size (20 by 20 m). Figure 5 shows the resulting land-use map. Four major types of land cover were identified as summarised in



Fig. 4 Photograph of one of the major landslides in the study area along the Prithvi highway; the landslide started in 2000 and was active several times in the next years; the picture was taken in 2003

Table 2. Almost half of the study area is used for agriculture; bush and forest make up the other half, while other land-uses as build-up areas are rare.

Unfortunately, there are no soil maps of Nepal. However, with the geological map of the region (Department of Geology and Mining, Nepal, 1981), the land-use map discussed above, aerial photographs of the Department of Survey, and reports from the Department of Roads, ten types of soils were identified in the study area, classified according to the Unified Soil Classification System. Obviously, the reliability of this map is questionable, but this was the best that could be done, since field reconnaissance to map soil types could not be pursued due to lack of resources and would anyway be very labourious and time consuming in this steep and rather inaccessible terrain. The percentage distribution covered by the different soil types is given in Table 3. A small portion of bare rock is excluded from the present analysis.

Rainfall data were obtained from the Department of Hydrology, Nepal. A 41-year long daily rainfall series recorded from 1956 to 1996 from a nearby meteorological station in Dhading Besi (valley) was selected to determine the magnitude–frequency relationships of extreme rainfall events. The rainfall data was analysed with the help of the DISTRIB model (Wanielista et al. 1997). Maximum daily rainfall values for various return periods were fitted with a log-normal distribution as shown in Fig. 6. From this fitted extreme value distribution, the expected maximum daily rainfall for a return period of 2 years can be estimated as about 100 mm/day. Caine and Mool (1982) and Pathak and Nilsen (2004) suggested that a rainfall intensity of 100 mm/day typically triggers landslides in Nepal. For a return period of 25 years the expected maximum daily rainfall is 235 mm; this is a rather extreme event but probable in the study area in such a time span.

Fig. 5 Land-use map of the study area

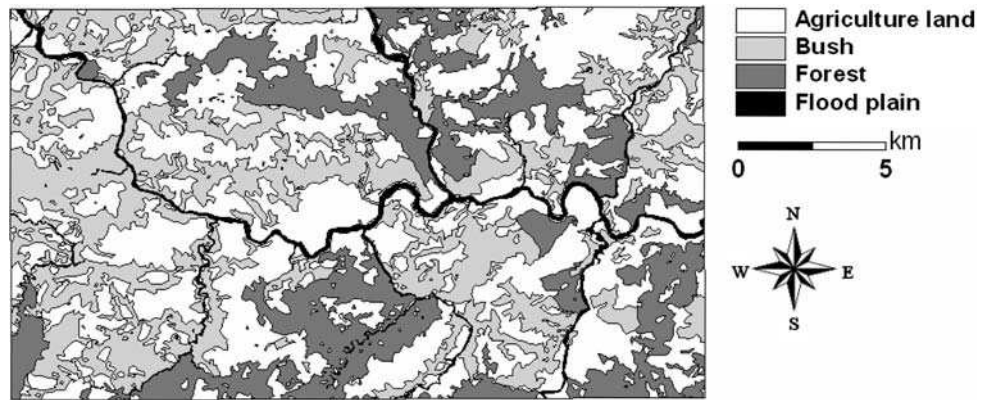


Table 2 Distribution of area (%) covered by different land-use classes

Land-use	Area (%)
Agricultural land	48.3
Bush	29.2
Forest	19.9
Flood plain/river	2.4
Other	0.2

Table 3 Distribution of area (%) covered by different soil types classified according to the Unified Soil Classification System

Soil type	Area (%)
SC: clayey sand	28.3
CL: sandy clay	13.8
GM: silty gravel	12.7
SP: poorly graded sand	12.1
ML: inorganic silt	10.1
SM: silty sand	9.9
GC: clayey gravel	8.1
GP: poorly graded gravel	4.1
OL: organic silt	0.7
Bare rock	0.2

Slope stability maps can be derived from the topography, land-use, soil types, and rainfall characteristics by simple GIS calculations using the equations given above. The calculation procedure is illustrated in Fig. 7. The DEM yields the slope angle, (θ), and the specific upstream contributing area for ground water flow (A_s). From the soil map, the hydraulic conductivity (K), soil cohesion (C_s), dry and saturated soil unit weight (γ_d and γ_s), and the soil friction angle (ϕ), can be determined based on literature and field experience. Soil cohesion and friction angle values were adapted from Deoja et al. (1991), and root cohesion from Sidle (1991). The hydraulic conductivity and soil density values were taken from Ingles and Metcalf

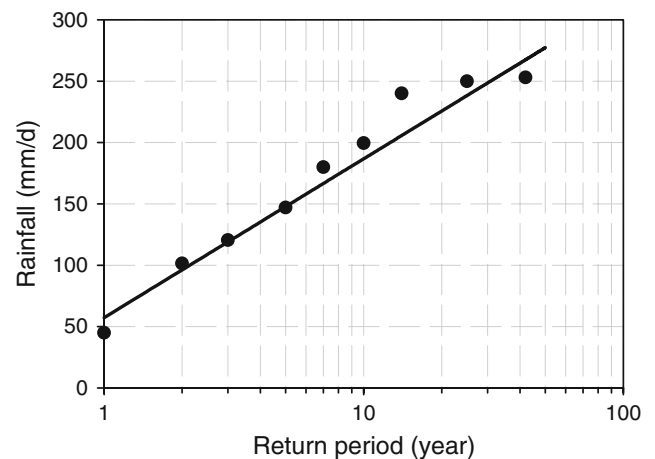


Fig. 6 Extreme rainfall distribution versus return period: observations are represented by *dots* and the fitted log-normal distribution by the *solid line*

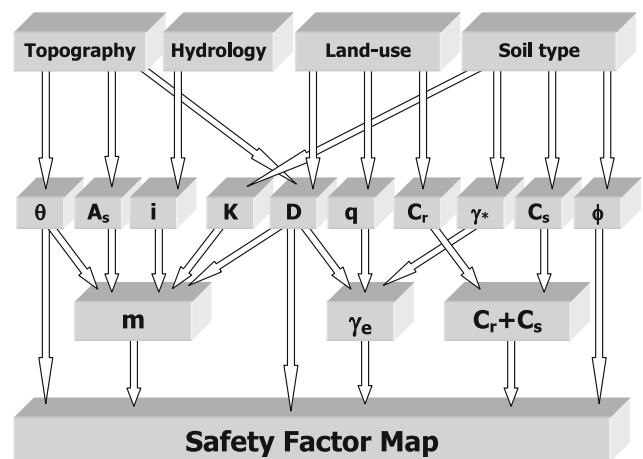


Fig. 7 Flow chart depicting the present methodology to derive slope stability safety factor maps from basic GIS data; all variables are explained in Eqs. 1–4; γ^* stands for γ_d and/or γ_s

(1972). The additional load on the soil surface (q) was estimated according to the prevailing land-use (Ray 2004). The depth of the soil above the bedrock or failure plane

was estimated from land-use and corrected for the slope angle, because depth of soil decreases with steepness of the terrain. Areas with grass and bush are thought to have limited root penetration depth, due to shallow underlying bedrock and, hence, the effective soil depth is assumed to be 1 m. On the other hand, agricultural land and built up area are thought to have a comparatively thicker depth of soil, assumed to be 2 m. Also, forest contains trees with high root penetration depth and, hence, is also assumed to have a soil depth of 2 m. These soil depth values were corrected slightly according to slope, i.e. for steep slope angles between 30° and 45° the soil depths were reduced by a factor 0.75, and for slope angles above 45° by 0.5. These are rather simplistic and crude assumptions which have not been verified in the field, but Acharya et al. (2006) have shown that the exact soil depth is not very critical for analysing slope stability, because it only has a limited influence on the cohesion effect but is unimportant for soil strength governed by friction.

Results and discussion

Five scenarios have been analysed including three under steady state conditions, assuming either completely dry soils, half saturated soils and fully saturated soil, and two under quasi-dynamic conditions, i.e. with soil wetness resulting from storm events with 2 and 25-year return periods. For the quasi-dynamic conditions, the soil wetness is either calculated based on the contributing area (Eq. 4) or on direct infiltration without contribution of subsurface water from neighbouring pixels (Eq. 5). The results are summarised in Table 4, showing the percentage of the different slope stability classes for each scenario.

The stability of a slope under dry conditions is only governed by soil cohesion, angle of internal friction, and surface slope. The results derived for this scenario provide the highest amount of land in stable condition (84.8%), 0.1% of the area as unstable, 2.2% as quasi stable and

Table 4 Distribution (%) of slope stability classes for the different scenarios

Scenario	Stable	Moderately stable	Quasi stable	Unstable
Dry ($m = 0$)	84.8	12.9	2.2	0.1
Half saturated ($m = 0.5$)	54.4	23.7	19.5	2.4
Saturated ($m = 1$)	29.4	17.4	27.8	25.4
2-year return period ^a	46.5	19.8	18.8	14.9
2-year return period ^b	37.6	23.0	27.5	11.9
25-year return period ^a	39.2	18.7	23.5	18.6
25-year return period ^b	30.5	18.3	27.1	24.1

^a Based on contributing area, Eq. 4

^b Based on local infiltration and storage, Eq. 5

12.9% as moderately stable. The percentage area with unstable and quasi-stable condition is still much less than the percentage of the study area with steep slope angles larger than 30°. Hence, most of the steep slopes are stable due to their mechanical properties (friction angle and soil and root cohesion). The small percentage of unstable slopes is clearly an artefact related to the limited validity of the underlying assumptions and input data, but since the predicted unstable area in dry condition is very small, the results are in accordance with expectations, i.e. in dry conditions all slopes should be stable.

The half saturation scenario yields very interesting and practical results. The distribution of the stability classes is shown in Fig. 8. Half saturation will likely occur, where there is a water table present and groundwater flow and/or infiltration occurs from rainfall events. Although it is not realistic to assume that every soil profile is exactly half saturated at the same time, this scenario gives a good idea of the distribution of the areas where landslides are more likely to occur. The results show that only 54.4% of the area is stable, and 23.7, 19.5 and 2.4% is moderately stable, quasi stable and unstable, respectively. Analysis of the relationship between slope angle and the half saturated

Fig. 8 Safety factor map for half saturated soil conditions (the circle in the middle indicates the site along the Prithvi highway where the landslide occurred, shown in Fig. 3)

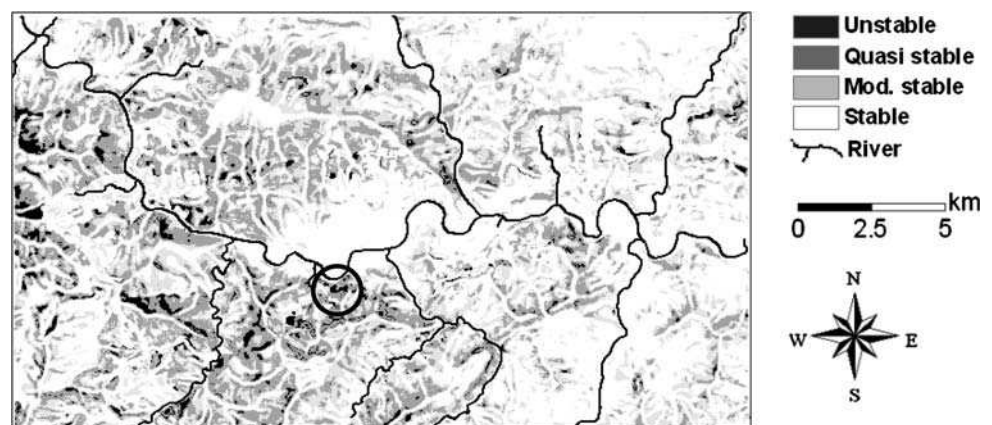


Fig. 9 Safety factor map for saturated soil conditions



safety factor indicates that the safety factor tends to be less than 1 mostly for agriculture lands on steep slopes, while areas with gentle slopes or with forest cover are generally stable or moderately stable. Additionally, most of the area along the Prithvi highway that was constructed by cutting the natural slope is found to be unstable or quasi stable, including the site at Krishna Bhir landslide shown in Fig. 4. However, these slopes have often been reinforced with gabions, or drained, which was not taken into account in the present analysis. This upgrading work has been generally successful.

Figure 9 shows the distribution of the stability classes for fully saturated conditions. In this case, 25.4% is unstable, 27.8% quasi stable, 17.4% moderately stable, and only 29.4% is stable. Most of the areas which are quasi stable under half saturated conditions become unstable when completely saturated. However, it is very uncommon to have complete soil saturation in mountainous area with steep slopes. Hence, this situation is rather hypothetical.

While comparing dry, half saturated, and saturated scenarios, one can clearly observe the effect of pore water pressure on slope stability. It is obvious that most slopes that are moderately stable under dry conditions become quasi stable in semi-saturated conditions and unstable when soils are fully saturated. Even more important is the effect of soil wetness on agricultural soils situated on steep slopes, where an increase in soil wetness can lead to instability. However, a drawback of these steady state scenarios is that no information can be obtained about rainfall characteristics that can trigger landslides and about the time (return) period in which such events can be expected to occur. Therefore, quasi-dynamic conditions resulting from storm events might give more useful information.

For dynamic conditions the soil saturation index can be calculated on the basis of the available rainfall data with Eq. 4 or 5. If the selected rainstorm lasts long enough for steady state groundwater flow conditions to prevail, the soil

saturation index can be predicted with Eq. 4. On the other hand, the use of Eq. 5 implies that the groundwater flow is slow and all the rainfall is first stored locally in the soil by a rise of the water table. Hence, the two methods constitute opposite situations. The stability classes are calculated with both methods for daily rainfall events of 103 and 235 mm, corresponding to return periods of 2 and 25 years, respectively. The results are given in Table 4. When comparing the two quasi-dynamic scenarios, it is found that the results are rather similar. The results of the two quasi-dynamic scenarios for both return periods are situated in between the results of the steady state half saturation and saturated scenarios. In particular, the results for the dynamic scenario based on infiltration and local storage in the soil by a rise of the water table for an extreme rainfall corresponding to a 25-years return period is almost identical to the steady state fully saturated scenario. This indicates that all soils would be nearly saturated by such an event. When the areas of unstable slopes are compared for the different methods, it is noted that the unstable slopes predicted by the local storage method nearly include all unstable slopes predicted by the groundwater flow contribution method, and are fully covered by the unstable slope areas predicted by the steady state saturation scenario. Hence, results based on the groundwater flow contribution method (Eq. 4) are less extreme and probably also less realistic. In fact, this approach is only suitable for small-scale study areas with steep slopes and permeable soils where ground water flow can quickly converge. The results from the local storage approach (Eq. 5) can be considered to be more realistic and reliable from the safety point of view.

Conclusions

Slope instability in steep mountainous terrain is a major concern. Gravitational slope failures can be triggered by

rainstorms when pore water pressures build up at the contact between the soil mantle and the underlying bedrock. In this study, a physically based slope stability spatial model combined with a hydrological model is presented and applied to a 350-km² area located in the Dhading district, Nepal. Three steady state scenarios (dry, half-saturated, and full-saturated soils) and also two quasi-dynamic scenarios (soil wetness resulting from daily rainfall events with return periods of 2 and 25 years) have been analysed. The quasi-dynamic scenarios have been based on either soil wetness resulting from accumulation of groundwater flow or from direct infiltration.

It can be concluded that, according to the models, only 29% of the soil-covered slopes in the study area are guaranteed to be stable under all conditions. These hillslopes are characterised by small slope angles. Soils that are unstable under fully saturated conditions are situated on steep slope angles with mostly agricultural land cover, or are excavated slopes along the highway. This indicates that these soils, due to their low cohesion and human disturbances become sensitive to failure with gradual increase of saturation.

For the quasi-dynamic scenarios, the wetness index is calculated with the equation developed by Montgomery and Dietrich (1994) based on the contributing area and compared to a new method based on local infiltration. The equation developed by Montgomery and Dietrich (1994) incorporates topographical as well as hydrological and hydrogeological characteristics of the study area. However, it neglects the time lag of the groundwater flow and, therefore, overestimates the impact of storm events producing results that do not differ much from the saturated scenario. On the other hand, the equation based on direct infiltration with the assumption of soils being initially saturated in some extent (half-saturated in this case), shows that the results strongly depend on the assumed initial wetness. Nevertheless, the results of this concept are found to be more reliable and realistic when compared to the results of the model based on contributing area.

In general the results indicate that agricultural land is particularly susceptible to slope failure. This is because cultivation usually starts after intense deforestation without constructing proper terraces even on steep slopes. This is one of the main reasons why, with every monsoon, properties and lives are lost due to slope failure. The present results might be helpful to provide information about landslide susceptibility to the concerned authorities, which would allow to setup warning systems or develop possible slope stability improvement measures to safeguard human welfare and sustainable development. However, the model validity has not been evaluated qualitatively with independent data. Hence, a thorough field investigation of past

and present landslides is needed first to verify the model predictions before any effective measures can be taken.

The proposed methodology for analysing landslide susceptibility on a regional scale, with basic data in GIS environment, may be useful for remote regions where detailed information is not available. However, the applied methodology has several limitations. The infinite slope method neglects the effects of failures of neighbouring pixels on the stability of the concerned pixel. Furthermore, the use of constant values for a particular parameter depending upon soil type or land cover does not correctly represent the actual spatial variability. Due to the lack of observed stability conditions and landslide occurrences in the field, calibration and quantitative validation of the model could not be pursued in this study. Consequently, we have no true information about the validity and predictive capability of our models.

Finally, it is recommended to carry out a detailed soil exploration and investigation in some areas identified as quasi stable and unstable under saturated condition and also to obtain more information on the hydrologic and hydrogeologic conditions during the dry season as well as in the rainy season, so that the analyses can be performed with more realistic groundwater data and less stringent assumptions.

References

- Acharya G, De Smedt F, Long NT (2006) Assessing landslide hazard in GIS: a case study from Rasuwa, Nepal. *Bull Eng Geol Environ* 65(1):99–107
- Aleotti P, Chowdhury R (1999) Landslide hazard assessment: summary review and new perspectives. *Bull Eng Geol Environ* 58(1):21–44
- Anbalagan R (1992) Landslide hazard evaluation and zonation mapping in mountainous terrain. *Eng Geol* 32(4):269–277
- Anbalagan R, Singh B (1996) Landslide hazard and risk assessment mapping of mountainous terrains: a case study from Kumaun Himalaya, India. *Eng Geol* 43(4):237–246
- Bonham-Carter GF (1994) Geographic information systems for geoscientists: modelling with GIS. Computer methods in the geosciences 13. Pergamon Press, Oxford, pp 398
- Borga M, Dalla Fontana G, Da Ros D, Marchi L (1998) Shallow landslide hazard assessment using physically based model and digital elevation data. *Environ Geol* 35(2–3):81–88
- Borga M, Dalla Fontana G, Cazorzi F (2002) Analysis of topographic and climatologic control on rainfall-triggered shallow landsliding using a quasi-dynamic wetness index. *J Hydrol* 268:56–71
- Burton A, Bathurst JC (1998) Physically based modelling of shallow landslide sediment yield at a catchment scale. *Environ Geol* 35(2–3):89–99
- Caine N, Mool PK (1982) Landslides in Kholpu-Khola drainage, Middle Mountains, Nepal. *Mt Res Dev* 2(2):157–173
- Carrara A, Cardinali M, Guzzetti F, Reichenbach P (1995) GIS technology in mapping landslide hazard. In: Carrara A, Guzzetti F (eds) *Geographical information systems in assessing natural hazards*. Kluwer, Dordrecht, pp 135–175

- Dahal RK (2004) Rainfall triggered landslides along roadside slopes of Nepal and their mitigation. Proceedings of 2nd one day international seminar on disaster mitigation in Nepal, Nepal Engineering College and Ehime University, Japan, pp 31–41
- Dahal RK, Hasegawa S, Masuda T, Yamanaka M (2006) Roadside slope failures in Nepal during torrential rainfall and their mitigation. In: Disaster mitigation of debris flows, slope failures and landslides, Universal Academic Press, Japan, pp 503–514
- Deoja BB, Dhital M, Thapa B, Wagner A (1991) Mountain risk engineering handbook. International Centre for Integrated Mountain Development (ICIMOD), Kathmandu, Nepal, pp 875
- De Smedt F (2006) Two- and three dimensional flow of groundwater. In: Delleur JW (ed) The handbook of groundwater engineering, second edition. CRC Press, pp 4.1–4.36
- Dhakal AS, Sidle RC (2004) Distributed simulation of landslides for different rainfall conditions. *Hydrol Process* 18:757–775
- Dhakal AS, Amada T, Aniya M (1999) Landslide mapping and the application of GIS in the Kulekhani watershed, Nepal. *Mt Res Dev* 19(1):3–16
- Dhital MR (2000) An overview of landslide hazard mapping and rating systems in Nepal. *J Nepal Geol Soc* 22:533–538
- Gorsevski PV, Gessler PE, Jankowski P (2003) Integrating a fuzzy k-means classification and a Bayesian approach for spatial prediction of landslide hazard. *J Geogr Syst* 5(3):223–251
- Guzzetti F, Carrara A, Cardinali M, Reichenbach P (1999) Landslide hazard evaluation: a review of current techniques and their application in a multi-scale study, Central Italy. *Geomorphology* 31(1–4):181–216
- Hansen A (1984) Landslide hazard analysis. In: Brunnsden D, Prior DB (eds) Slope instability. Wiley and Sons, New York, pp 523–602
- Hutchinson JN (1995) Keynote paper: landslide hazard assessment. In: Bell DH (ed) Landslides, proceeding of VI international symposium on landslides, Christchurch, New Zealand, pp 1805–1841
- Ingles OG, Metcalf JB (1972) Soil stabilization—principles and practice. Butterworth, Sydney, pp 374
- Joshi J, Majtan S, Morita K, Omura H (2000) Landslide hazard mapping in the Nallu Khola watershed, Central Nepal. *J Nepal Geol Soc* 21:21–28
- Montgomery DR, Dietrich WE (1994) A physically based model for the topographic control on shallow landsliding. *Water Resour Res* 30(4):1153–1171
- Pack RT, Tarboton DG, Goodwin CN (1998) The SINMAP approach to terrain stability mapping. In: Moore DP, Hungr O (eds) Proceedings international congress of the international association for engineering geology and the environment 8(2), A.A. Balkema, Rotterdam, Netherlands, pp 1157–1165
- Pack RT, Tarboton DG, Goodwin CN (2001) Assessing terrain stability in a GIS using SINMAP. Paper presented at the 15th annual GIS conference, GIS 2001, Vancouver, British Columbia, 19–22 February 2001
- Pathak S, Nilsen B (2004) Probabilistic rock slope stability analysis for Himalayan condition. *Bull Eng Geol Environ* 63:25–32
- Petley DN, Hearn GJ, Hart A (2004) Towards the development of a landslide risk assessment for rural roads in Nepal. In: Glade T, Crozier MJ (eds) Landslide hazard and risk. Wiley and Sons, London, pp 597–679
- Ray RL (2004) Slope stability analysis using GIS on a regional scale: a case study from Dhading, Nepal. MSc, Vrije Universiteit Brussel, Belgium
- Saha AK, Gupta RP, Arora MK (2002) GIS-based landslide hazard zonation in the Bhagirathi (Ganga) Valley, Himalayas. *Int J Remote Sens* 23(2):357–369
- Sarkar S, Kanungo DP (2004) An integrated approach for landslide susceptibility mapping using remote sensing and GIS. *Photogramm Eng Remote Sens* 70(5):617–625
- Sidle RC (1991) A conceptual model of changes in root cohesion in response to vegetation management. *J Environ Qual* 20(1):43–52
- Skempton AW, DeLory FA (1957) Stability of natural slopes in London clay. Proceedings 4th international conference on soil mechanics and foundation engineering 2:378–381
- Skirikar SM, Rimal LN, Jäger S (1998) Landslide hazard mapping of Phewa Lake catchment area, Pokhara, Central West Nepal. *J Nepal Geol Soc* 18:335–345
- Soeters R, van Westen CJ (1996) Slope instability recognition, analysis and zonation. In: Turner KT, Schuster RL (eds) Landslide: investigation and mitigation. Spec Rep 47. Transportation Research Board, National Research Council, Washington DC, pp 129–177
- Thapa PB, Dhital MR (2000) Landslide and debris flows of 19–21 July 1993 in the Agra Khola Watershed of Central Nepal. *J Nepal Geol Soc* 21:5–20
- van Westen CJ (1994) GIS in landslide hazard zonation: a review, with examples from the Andes of Colombia. In: Price MF, Heywood DI (eds) Mountain environments and geographic information systems. Taylor and Francis Publishers, London, pp 135–165
- van Westen CJ, Terlien TJ (1996) An approach towards deterministic landslide hazard analysis in GIS: a case study from Manizales (Colombia). *Earth Surf Process Landf* 21:853–868
- van Westen CJ, Rengers N, Terlien MTJ, Soeters R (1997) Prediction of the occurrence of slope instability phenomena through GIS-based hazard zonation. *Geol Rundsch* 86(2):404–414
- Varnes DJ (1984) Landslide Hazard Zonation: a review of principles and practice. Commission on the landslides of the IAEG, UNESCO, Natural Hazard 3:66 pp
- Wanielista M, Kersten R, Eaglin R (1997) Hydrology: water quantity and quality control. Wiley and Sons, New York, pp 567
- Windisch EJ (1991) The hydraulics problem in slope stability analysis. *Can Geotech J* 28(6):903–909